Advanced Phase Rotation Unit Cells for Beam Steering and Polarization Conversion with Enhanced Sidelobe Performance

Arun T. Raveendran*, Khushboo Singh*, Dushmantha N. Thalakotuna*, Karu P. Esselle*, and Syed Muzahir Abbas†
* The University of Technology Sydney, 15 Broadway, Ultimo NSW 2007, Australia
arun.t.raveendran@student.uts.edu.au
† GME, Winston Hills, NSW 2153 Australia

***Abstract*—This paper analyzes a phase rotation unit cell intended for circular polarization conversion and sidelobe suppression in metasurface-based antenna systems. The proposed structure leverages Pancharatnam–Berry phase principles to achieve continuous 360° phase coverage through unit cell rotation. The unit cell effectively converts the LHCP excitation to RHCP with high transmission efficiency, which is validated through full-wave electromagnetic simulations over the 12.5–14.5GHz frequency band. The S-parameter results confirm efficient polarization conversion performance, with S_{21}^{RHCP} ranging from –1 to –2.5dB, S_{21}^{LHCP} remaining below –8dB, and S_{11}^{LHCP} below –8dB across all rotation states. The design maintains consistent phase shift characteristics and polarization purity, enabling precise wavefront manipulation. The supercell-level analysis further demonstrates an average back lobe suppression of 2dB without compromising broadside radiation. These results highlight the effectiveness of unit cell level optimization in improving array performance while reducing the need for complex array level compensation strategies.**

***Index Terms*—Phase rotation cells, phase delay cells, Pancharatnam–Berry Phase, Phase gradient metasurface, Transmitarray, Reflectarray, Polarization conversion, Beam steering, .**

I. Introduction

RECENT evolutions in modern communication systems and radar technologies urgently require high-performance antennas with capabilities in precision beam control, enhanced polarization capability, and compact, lightweight design. These are essential in applications ranging from satellite communications to vehicular connectivity, where high gain, wide bandwidth, and reliable polarization performance are critical. Some significant drawbacks in conventional high-gain antennas, including phased arrays and parabolic reflectors, relate to complex high-profile configurations and elaborative feed networks with potential increases in system cost in most cases [1]- [2].

Circularly polarized (CP) antennas have become a cornerstone for these systems due to their ability to mitigate polarization mismatches, reduce multipath fading, and provide resilience in dynamic environments. However, realizing wideband circular polarization and independent polarization control within a compact form factor remains a big challenge. Recent breakthroughs in metasurface technologies have presented innovative solutions using subwavelength unit cells to manipulate electromagnetic wavefronts rapidly. Such unit cells can enable functionalities like beam steering, polarization conversion, and multi-band operation, which are not achievable by conventional antenna designs [3].

Phase delay (PD) and phase rotation (PR) are the two main phase control methods used for wavefront manipulation in metasurface-based antennas. The PD cells will modulate the phase by controlling the effective electrical length of the unit cell, which is commonly done by altering the geometry or material properties. Unlike PD cells, PR cells achieve phase shifts through the physical rotation of anisotropic elements, a straightforward and easy process utilizing the Pancharatnam–Berry (PB) phase principle [4]. The advantages mentioned above motivate the selection of PR cells for this study. The focus here is on optimizing the performance of the individual unit cell to minimize sidelobes rather than applying computationally intensive corrections at the supercell or array level.

The PR unit cell technology has emerged as a breakthrough in developing metasurfaces, reflectarrays, and transmitarrays by offering continuous phase control in the framework of beam steering or polarization conversion [5]. Nevertheless, all PR cell designs suffer from unsolved issues such as high sidelobe levels, unbalanced phases, deteriorations under oblique incidence, and several other limitations, which practically inhibit the full exploitation of PR cells within real antenna systems.

Previous studies have mainly concentrated on enhancing performance, such as beam steering and polarization conversion at the array or supercell levels [6]- [8]. There has been limited exploration into optimizing unit cell characteristics to affect the sidelobe behavior at the array level, even though such strategies can significantly improve the overall radiation quality of metasurface-based antennas.

The proposed research focuses on designing and optimizing single-band PR unit cells capable of transforming left-hand circular polarization (LHCP) to right-hand circular polarization (RHCP) and vice versa. A single-band approach simplifies the design without sacrificing much of its performance. Hence, it can be suitable for applications where the size, weight, and cost are rigid constraints, like satellite and vehicular communication systems.

The rest of the paper is organized as follows: Section II

presents the theoretical background, design principles and methodologies of PR unit cells, key design parameters, and techniques for achieving desired phase rotation combined with polarization conversion. Section III presents the full-wave simulation results of the proposed PR unit cell, including its beam-steering, polarization conversion, and sidelobe performance, along with supercell-level analysis. Section IV presents the conclusion, outlining the key findings of this analysis and providing guidance for future work.

II. Design Principles and Methodologies of PR Unit Cells

Modern antenna systems use numerous technologies to enhance performance, but PR cells are less explored. The PR unit cells' geometric design and orientation enable them to produce different phase changes across incident electromagnetic waves. The ability to control phases is most valuable for metasurface, reflectarray, and transmitarray antennas, which require precise wavefront shaping functions.

In circularly polarized antennas, PR unit cells enable the conversion between LHCP and RHCP. This unit cell acts as a polarization transformer using anisotropic or rotationally symmetric structures that enable polarization conversion and spatial phase variation in the transmitted wave. The mathematical framework underlying PR unit cells is primarily based on the PB phase, which is described as [9] :

$$\phi = 2\alpha \tag{1}$$

where α represents the rotation angle of the unit cell structure. This relationship allows a complete $0^\circ - 360^\circ$ phase shift range to be achieved by simply adjusting the rotational orientation of the unit cell.

Additionally, PR unit cells can be analyzed using transmission matrices, where the matrix representation defines the transformation of incident polarization states. For an ideal PR cell, the transformation matrix for circular polarization is given by:

$$T_{PR} = \begin{bmatrix} e^{j\phi} & 0 \\ 0 & e^{-j\phi} \end{bmatrix} \tag{2}$$

This matrix indicates that a phase shift ϕ is imparted to one polarization component while an opposite phase shift $-\phi$ is applied to the orthogonal component.

The structure under consideration, chosen from an already published paper [4], consists of three metallic layers and two dielectric layers. The top and bottom metallic layers are identical, featuring a rectangular patch embedded within a split-ring structure. This configuration enables controlled phase shifts through the orientation of these patches. The middle metallic layer, depicted in Figure 2, consists of a rectangular strip inside a circular slot. The rotation angle directly determines the phase shift imparted by the unit cell according to the PB phase principle.

The choice of dielectric substrate significantly influences the performance of the unit cells. Rogers RT5880 is a common low-loss substrate with a dielectric constant of 2.2 and a low-loss of 0.001. It is ideal for applications that require high efficiency and low insertion loss. This substrate promotes stable electromagnetic properties across a wider frequency range, resulting in improved phase stability and transmission performance. The design of patterned metallic patches needs extreme precision to reduce resistive losses and maintain high conductivity for improved efficiency. The values of the variables marked in Figure 1 and Figure 2 are described in Table I. The overall performance of the unit cell depends on minimizing cross-polarization effects and maximizing transmission efficiency, depending on the intended application.

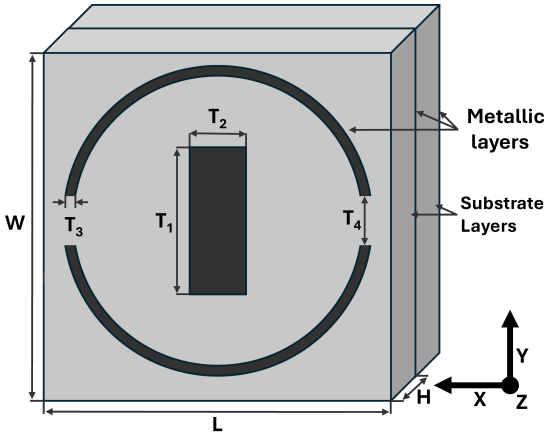

Fig. 1. Geometric configuration of the proposed PR unit cell.

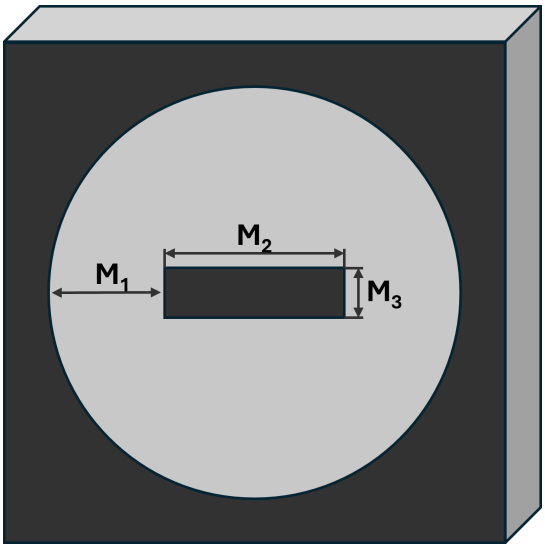

Fig. 2. Middle layer of the PR unit cell with dimension.

TABLE I
Geometrical Parameters of the Proposed PR Unit Cell.

Variable	Value (mm)	Variable	Value (mm)
L	11.1	T_3	0.334
W	11.1	T_4	2.290
H	1.575	M_1	3.350
T_1	6.184	M_2	2.950
T_2	2.941	M_3	0.782

III. Results and Discussion

In this section, a detailed analysis of the electromagnetic performance of the PR unit cell is presented. The goals to be achieved with this unit cell are effective beam steering, polarization conversion, and improved sidelobe suppression. The analysis is carried out using CST Studio Suite, applying periodic boundary conditions and Floquet ports to model realistic operation scenarios of the unit cell. Key parameters, including transmission efficiency, phase characteristics, and co and cross-polarized directivities, are analyzed by varying the angular orientation of the unit cell from 0° to 150° with a step of 30°(0°, 30°, 60°, 90°, 120°, and 150°). The performance of the sidelobe at the array level is also carefully studied to show how well the proposed PR unit cell reduces unwanted radiation.

A. Unit Cell Performance and Polarization Conversion Analysis

The polarization conversion efficiency of the unit cell can be analyzed by evaluating the transmission coefficient for the LHCP input to the RHCP output (S_{21}^{RHCP}). Figure 3 shows that the S_{21}^{RHCP} magnitude consistently remains between -1 dB and -2.5 dB across the entire operating frequency range (12.5–14.5 GHz) for all rotation angles. Such high transmission indicates that most of the input LHCP wave is successfully converted into RHCP, confirming the unit cell's effective polarization-conversion capability and potential for use in polarization-sensitive antenna systems and applications.

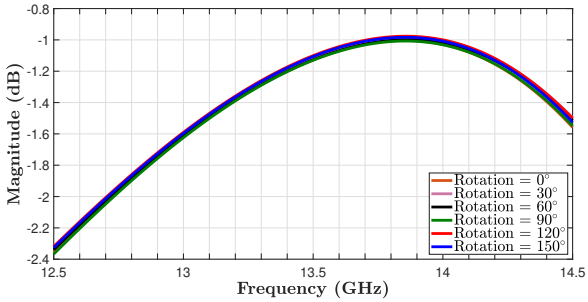

Fig. 3. Simulated transmission coefficient S_{21}^{RHCP} of PR unit cell across different rotation angles from 0° to 150° at a step of 30°.

Figure 4 shows the reflection coefficient for the LHCP input and LHCP output(S_{11}^{LHCP}), which is analyzed to verify impedance matching and reflection behavior. Across the operating frequency range, S_{11}^{LHCP} remains consistently below approximately -8 dB for all unit cell rotation angles. This indicates effective impedance matching, as very little of the incoming LHCP wave is reflected. Although minor variations are visible at different rotation angles, the overall reflection performance remains stable and within acceptable limits. This stability ensures the reliable operation of the unit cell in practical antenna configurations and confirms that the designed structure effectively supports efficient power transfer to the transmitted polarization state.

Figure 5 shows the transmission coefficient for LHCP transmission (S_{21}^{LHCP}), representing the undesired polarization

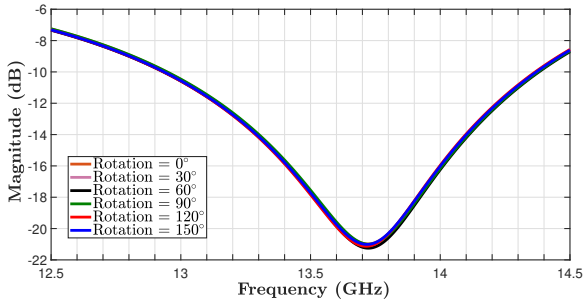

Fig. 4. Simulated reflection coefficient S_{11}^{LHCP} of PR unit cell across different rotation angles from 0° to 150° at a step of 30°.

leakage. Across the frequency range, the magnitude remains consistently below approximately -8 dB at all rotation angles. Such low values indicate very effective suppression of unwanted cross-polarized transmission (in this case LHCP to LHCP), thereby confirming excellent polarization purity.

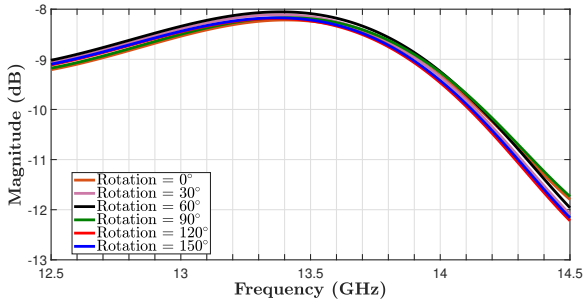

Fig. 5. Simulated transmission coefficient S_{21}^{LHCP} of PR unit cell across different rotation angles from 0° to 150° at a step of 30°.

Figure 6 shows the simulated phase shift ($\angle S_{21}^{\mathrm{RHCP}}$) for different rotation angles of the PR unit cell over the entire frequency band. At a frequency of 13.5 GHz, the phase response progresses smoothly from approximately 6.9° (0° rotation) to 306.2° (150° rotation), almost covering the full 360° range.

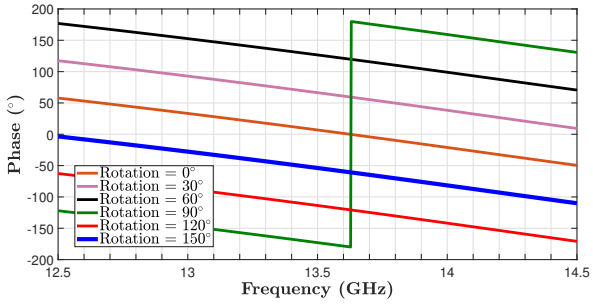

Fig. 6. Simulated transmission phase ($\angle S_{21}^{\mathrm{RHCP}}$) of PR unit cell across different rotation angles from 0° to 150° at a step of 30°.

This continuous and monotonic phase variation with increasing rotation angle confirms the capability of the PR unit cell to manipulate the transmitted wavefront effectively. According to the PB phase principle, the anisotropic scatterer

achieves phase shifts equal to twice the rotation angle. The unit cell rotation in this design directly controls the phase shift of transmitted waves, which creates linear phase responses in array configurations. Such characteristics are suitable for beam steering and wavefront engineering applications with precise phase control. Additionally, the phase remains stable across the frequency band for each rotation angle, confirming broadband performance.

B. Supercell Design and Radiation Pattern Analysis Using Array Theory

The far-field radiation characteristics of the unit cell were evaluated by plotting the co-polarized (LHCP to RHCP, desired) and cross-polarized (LHCP to LHCP, undesired) directivity responses over the complete frequency range, as shown in Figure 7. At the center frequency of 13.5 GHz, the co-polarized directivity(converted) remains high, reaching approximately 3.9 dB, while the cross-polarized directivity(non-converted) is significantly lower, around -3.2 dB along the broadside. This behavior confirms that the unit cell effectively converts the incident LHCP wave into the desired RHCP wave with strong polarization purity. Similarly, the consistency across the entire band demonstrates that this performance is maintained throughout the operational bandwidth.

To evaluate the performance of the unit cell in an array configuration, a linear supercell composed of 12 elements was modeled, as shown in Figure 8. Each unit cell is rotated to create a fixed phase shift of 60° between adjacent elements, according to the PB phase mechanism. This engineered phase gradient enables beam steering toward a desired angle. The supercell design introduces a progressive phase shift across the array aperture. This phase gradient facilitates constructive interference in the desired direction and destructive interference in the sidelobe regions. This progressive phase distribution enables beam steering by manipulating the interference pattern of the transmitted wavefronts. The required phase difference $\Delta\phi$ between adjacent unit cells for steering the main beam toward an angle θ is calculated using classical array theory [6]:

$$\Delta\phi = \frac{2\pi}{\lambda} d \sin(\theta) \tag{3}$$

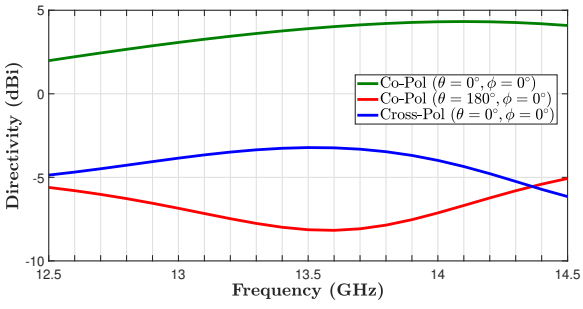

Fig. 7. Simulated co-polarized directivity (LHCP → RHCP) at $\theta = 0°$ and $\theta = 180°$, and cross-polarized directivity (LHCP → LHCP) at $\theta = 0°$, all evaluated at $\phi = 0°$.

Where λ is the wavelength at the operating frequency, and d is the spacing between adjacent unit cells. In this design, the spacing between elements is set to $\lambda/2$, and each unit cell introduces a phase shift of 60°.This configuration allows the supercell to direct the main beam at approximately 19.5°, confirming the effectiveness of the unit-cell-level phase control strategy.

Fig. 8. Three-dimensional view of the 1×12 supercell array, composed of optimized PR unit cells with an incremental 30° rotation between adjacent elements along the x-axis.

A supercell configuration was designed to evaluate the impact of unit cell-level optimization on array-level radiation performance by replicating the optimized unit cell in a linear 1×12 array. Using CST Microwave Studio, the RHCP directivity of the array was simulated using the array factor method. Far-field analysis was performed for both broadside ($\theta = 19.5°$) and backlobe ($\theta = 180°$) directions to assess radiation behavior in the operational frequency range.

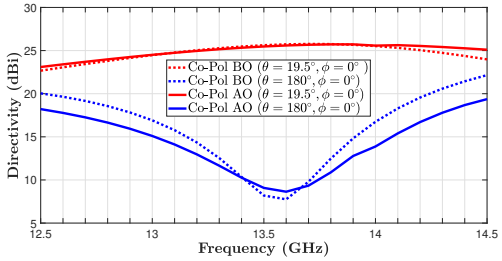

Fig. 9. Comparison of simulated RHCP directivity at broadside ($\theta = 19.5°$) and backlobe direction ($\theta = 180°$) of the array before and after unit cell-level optimization.

Figure 9 present the RHCP directivity at the broadside ($\theta = 19.5°$) and back lobe ($\theta = 180°°$) directions before and after optimization. On the broadside, the optimized design (green curve) demonstrates an improved peak directivity of approximately 25.1dB compared to 23.97dB in the unoptimized case. The back lobe directivity significantly decreased from 22.15 dB to 19.37 dB, resulting in an average sidelobe suppression of approximately 2.8 dB. This enhancement verifies the effectiveness of optimizing at the unit cell level to shape the array radiation pattern, thereby reducing backlobes while maintaining broadside gain. These results highlight the potential of optimizing polarization conversion unit cells to achieve improved far-field performance at the metasurface level without depending on complex array-level synthesis techniques.

This improvement results from better current flow and accurate phase control at the unit cell level, which leads to more focused and consistent radiation when the cells are used in an array. The accompanying simulation results, including the variation of phase, far-field co-polarized and cross-polarized directivity patterns, and the stability of RHCP transmission at the broadside across all rotation states, collectively validate the unit cell's angular response, polarization conversion efficiency,

and consistent phase behavior across the operating frequency range. These results confirm that the optimized unit cell provides efficient polarization conversion and complete phase coverage and contributes significantly to sidelobe suppression. This demonstrates that sidelobe reduction can be effectively addressed at the unit cell level by minimizing the need for complex compensation techniques at the array level and simplifying the overall design of metasurface-based antenna systems. A comparative analysis of the existing paper and available unit cells is explained in Table II.

TABLE II
COMPARISON OF PR UNIT CELLS WITH POLARIZATION CONVERSION

Ref.	Pol. Conv.	Freq. (GHz)	S_{21} (dB)	S_{11} (dB)
This Work	LHCP $\leftrightarrow$ RHCP	12.5–14.5	<–1	< –8
[5]	LHCP $\leftrightarrow$ RHCP	16–18	<–1	<–10
[10]	LHCP $\leftrightarrow$ RHCP (Dual-band)	16–20 20–24	< –2	< –10
[11]	LHCP $\rightarrow$ RHCP	50–70	< –1.5	< –10

IV. CONCLUSION

In this work, a phase rotation unit cell was evaluated for circular polarization conversion and sidelobe suppression. The unit cell achieves efficient LHCP to RHCP transmission with low reflection and minimal cross-polarized leakage, as verified through S-parameter analysis across the 12.5–14.5GHz band. The unit cell also provides a smooth phase shift under rotation, confirming its suitability for wavefront manipulation and beam steering. Supercell-level radiation analysis further confirms that unit cell-level optimization improves radiation performance, achieving approximately 2dB back lobe suppression while maintaining stable broadside gain. These results show that key performance parameters, such as polarization purity and sidelobe levels, can be effectively controlled at the unit cell stage without requiring additional array-level compensation techniques.

ACKNOWLEDGEMENT

This work was supported by the SmartSat Cooperative Research Center (CRC) under the Australian Government Cooperative Research Center Program..

REFERENCES

[1] P. Wang *et al.*, "Dual-Band Dual-Circularly Polarized Fabry-Pérot Cavity MIMO Antenna Using CMM-Based Polarization Converter and MMA for Vehicular Satellite Communications," *IEEE Transactions on Vehicular Technology*, vol. 72, no. 7, pp. 8844–8856, Jul. 2023.

[2] R. Madi, A. Clemente, and R. Sauleau, "Dual-Band, Dual-Linearly Polarized Transmitarrays for SATCOM Applications at Ka-Band," in *Proc. 16th European Conference on Antennas and Propagation (EuCAP)*, 2022, pp. 1–4.

[3] M. U. Afzal, A. Lalbakhsh, and K. P. Esselle, "Method to Enhance Directional Propagation of Circularly Polarized Antennas by Making Near-Electric Field Phase More Uniform," *IEEE Transactions on Antennas and Propagation*, vol. 69, no. 8, pp. 4447–4456, Aug. 2021.

[4] P. Naseri *et al.*, "Phase-Delay Versus Phase-Rotation Cells for Circular Polarization Transmit Arrays—Application to Satellite Ka-Band Beam Steering," *IEEE Transactions on Antennas and Propagation*, vol. 66, no. 3, Mar. 2018.

[5] L. Haoyu *et al.*, "A Low-Profile Risley-Prism-Based 2-D Beam-Scanning Circularly Polarized Folded Transmitarray Antenna at Ku-Band," *IEEE Trans. Antennas Propag.*, vol. 71, issue. 7, pp. 6173–6178, Jul. 2023.

[6] K. Singh *et al.*, "Controlling the Most Significant Grating Lobes in Two-Dimensional Beam-Steering Systems With Phase-Gradient Metasurfaces," *IEEE Transactions on Antennas and Propagation*, vol. 68, issue 3, pp. 1389–1401, Mar. 2020.

[7] K. Singh *et al.*, "Suppressing Sidelobes in Metasurface-Based Antennas Using a Cross-Entropy Method Variant and Full Wave Electromagnetic Simulations," *Electronics*, vol. 12, no. 20, p. 4229, Oct. 2023.

[8] K. Singh*et al.*, "Optimizing amplitude distribution in a feed array to control side-lobe levels of a beam-steering metasurface," in *Proc. URSI Int. Symp. Electromagn. Theory (EMTS)*, pp. 1–4, May 2019.

[9] P. Naseri, F. Khosravi, and P. Mousavi, "Antenna-Filter-Antenna-Based Transmit-Array for Circular Polarization Application," *IEEE Antennas and Wireless Propagation Letters*, vol. 16, pp. 1389–1392, 2017.

[10] W. Yang *et al.*, "Frequency-Multiplexed Spin-Decoupled Metasurface for Low-Profile Dual-Band Dual-Circularly Polarized Transmitarray With Independent Beams," *IEEE Transactions on Antennas and Propagation*, vol. 72, no. 1, pp. 642–652, Jan. 2024.

[11] C. Yang *et al.*, "An Ultralow-Profile Folded Transmitarray Antenna Based on a Multifunctional Metasurface With Both-Sided Wavefront Control," *IEEE Transactions on Antennas and Propagation*, vol. 71, no. 10, pp. 7804–7812, Oct. 2023.